PAPER

Laser frequency stabilization in sub-nanowatt level using nanofibers

IOP Publishing Journal of Physics D: Applied Physics
J. Phys. D: Appl. Phys. **51** (2018) 465001 (5pp) https://doi.org/10.1088/1361-6463/aae2f8

Laser frequency stabilization in sub-nanowatt level using nanofibers

Dian-Qiang Su[1,2], Rui-Juan Liu[1,2], Chuan-Biao Zhang[1,2], Zhong-Hua Ji[1,2], Yan-Ting Zhao[1,2], Lian-Tuan Xiao[1,2] and Suo-Tang Jia[1,2]

[1] State Key Laboratory of Quantum Optics and Quantum Optics Devices, Institute of Laser Spectroscopy, Shanxi University, Taiyuan 030006, People's Republic of China
[2] Collaborative Innovation Center of Extreme Optics, Shanxi University, Taiyuan 030006, People's Republic of China

E-mail: zhaoyt@sxu.edu.cn

Received 26 June 2018, revised 6 September 2018
Accepted for publication 20 September 2018
Published 5 October 2018

Abstract

We introduce a novel scheme which combines conventional Doppler dichroic atomic vapor laser lock (DAVLL) and nanofiber techniques for realizing frequency stabilization with sub-nanowatt laser power. The dependences of DAVLL signal on the total incident power of probe light and the quantification magnetic field amplitude indicate that the power for frequency stabilization could be minimized to only 15 pW. To evaluate the frequency stability of the locked laser, we calculate the Allan standard deviation, which shows that the relative frequency stability could reach 10^{-10} level at 10 s. This frequency stabilization scheme paves the road for future quantum optical device integration.

Keywords: sub-nanowatt, frequency stabilization, nanofiber

(Some figures may appear in colour only in the online journal)

1. Introduction

There have been significant developments in integrated optics recently due to the advances in manufacturing and data processing. The integrated laser is realized by coupling the low-loss silicon nitride waveguides to a gain chip, which extremely contributes to the narrow linewidth compacted laser [1]. The integrated Bragg grating not only solves the spectral filtering problem but also can be used to process the photonic signal in optical circuits [2]. Optical-frequency synthesizers and ultra-low-loss resonators [3, 4] are also developed for future photonic circuits and systems. However, for the laser frequency stabilization system, conventional techniques including modulation [5–8] or modulation-free [9–12] schemes are not appropriate for the applications in optical system integration. There are still needs to minimize the system size for the integrated applications in future.

Recently, the emergence of tapered optical nanofiber provides a potential solution. The nanofiber can be manufactured using the 'flame-brush' technique [13–15] and the minimum diameter of nanofiber can reach to several hundreds of nanometer. The high temperature flame out of hydrogen and oxygen burning melts the glass of standard single-mode fiber and ensures the low surface roughness of the nanofiber. Optimized stretching algorithm results in the unique geometry to guarantee the adiabatic transformations of fiber-guided light between multi-mode and single mode, which plays a crucial role in avoiding the 'refraction leak' from the nanofiber. In free space, the laser is hard to be focused to 1 μm in diameter and the length maintaining focused diameter would be limited by the divergence of Gauss beam. However, the tightly confined evanescent field around the nanofiber which has a 500 nm in diameter and a tapper length over 3 mm makes it promising in atom-light interactions with ultra-low power [16, 17]. The evanescent field could strongly modify the spontaneous decay rate [18] induced by the changed photon transport properties [19, 20]. It can also be used for sensing the van der Waals potential arising from the nanofiber surface [21]. In addition, the nanofibers could be exploited to construct a one-dimensional optical lattice for atomic trapping and provide a platform for chiral quantum optics [22, 23]. Seminal works are accomplished by using 'magic' wavelengths for the trapping fields including red and blue-detuned lights [24]. At most one atom can be loaded per site of the lattice owing to

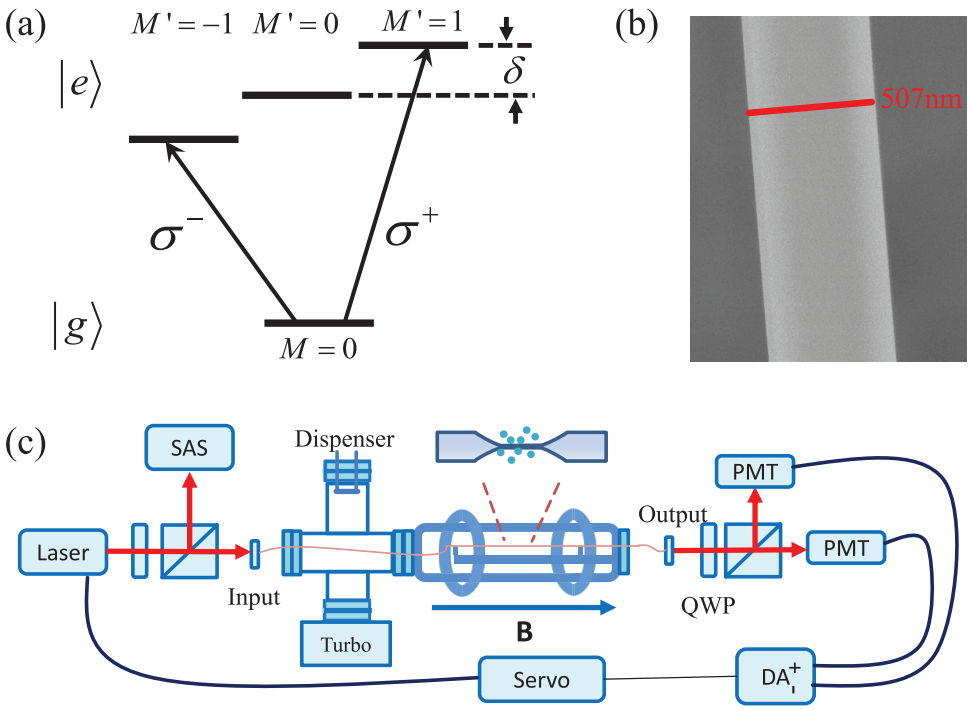

Figure 1. (a) Simplified relevant energy levels. In presence of axial quantification magnetic field, the excited state $|e\rangle$ is degenerated into three levels due to the Zeeman splitting. The excited states $|M' = -1\rangle$ and $|M' = +1\rangle$ are separately coupled to ground state $|g\rangle$ via σ^- and σ^+ transitions. (b) The image of tapered nanofiber obtained by scanning electron microscope. (c) Diagram of the ultra-low power frequency stabilization scheme. PMT, photomultiplier tube; QWP, quarter-wave plate; DA, differential amplifier; SAS, saturated absorption spectroscopy.

the collisional blockade effect during the loading stage [25]. Based on the large optical depth, optical memories are also realized [26, 27]. The demonstrations of atomic mirror through ordered atom chain trapped by the optical lattice contribute to applications in quantum network and many-body effects [28, 29]. Whispering-gallery-mode microresonators [30] and photonic crystals waveguide based on nanofibers [31, 32] indicate the potential in integrated optics for the nanofiber.

On the other side, lots of works have been done with frequency locking techniques using the modest optical power [6–12]. To realize the frequency stabilization with ultra-low power, we introduce a new scheme which combines the Doppler dichroic atomic vapor laser lock (DAVLL) and nanofiber techniques. In this scheme, the power needed to lock the frequency is only tens of picowatts due to the tight transverse confinement of evanescent field around the nanofiber. It also enables the applications for future photonic integration circuits in frequency stabilization system.

2. Methods

Figure 1(a) shows a simplified atomic energy level diagram. The excited levels $|M' = -1\rangle$ and $|M' = +1\rangle$ are separately coupled to ground state $|g\rangle$ via σ^- and σ^+ transitions. In presence of a weak magnetic field, the Zeeman splitting can be written as:

$$\Delta E = \mu_B g_F B_Z, \tag{1}$$

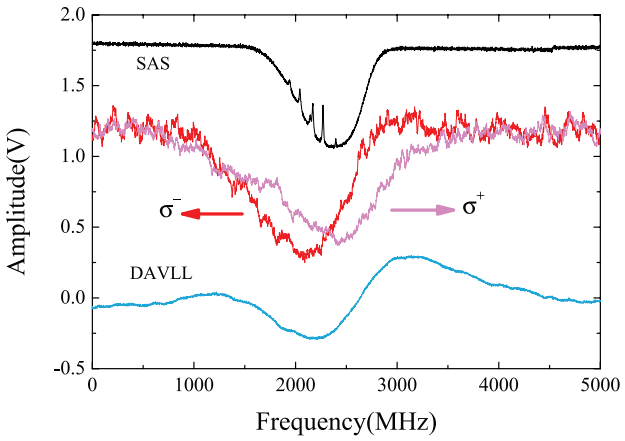

Figure 2. Filtered DAVLL signal of cesium D_2 transition $F = 4 \rightarrow F'$ indicated by the blue line corresponding to the 90 pW of total incident power of probe light and 70 G of magnetic field. The two circularly polarized components σ^+ and σ^- are separately shown by pink and red lines. The SAS plays a role in frequency scaling.

where g_F is the Landé g-factor of hyperfine excited state and μ_B is Bohr magneton.

The tapered optical nanofibers we exploit in experiment are stretched from standard single-mode fiber (Fiber Core SM800 5.6/125) using the classical 'flame-brush' technique [13–15]. The specially designed 'U-shape' structure in tapered region contributes to the high transmission and short stretching length in total 'brush' progress. According to the tests from

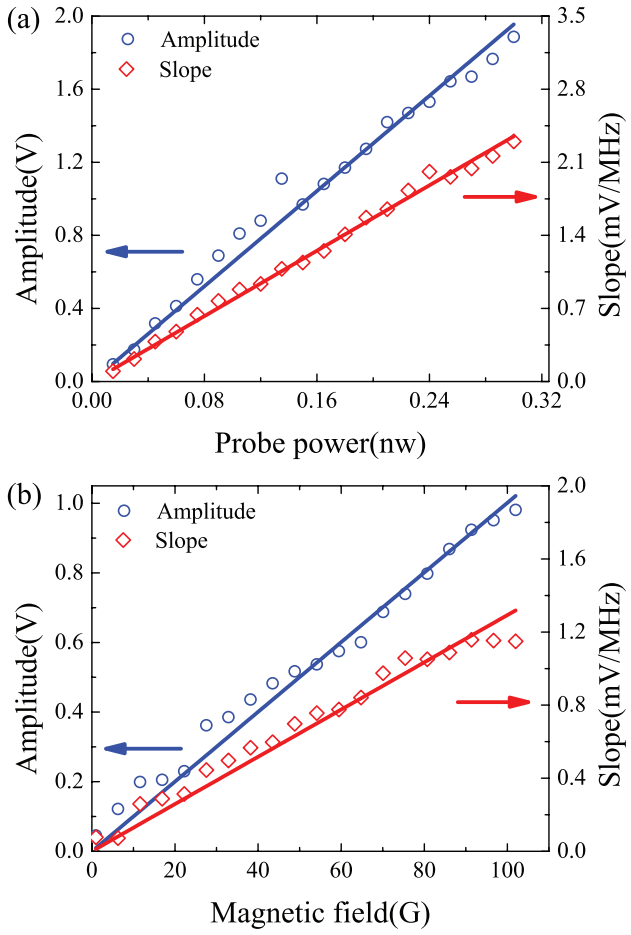

Figure 3. (a) Dependences of DAVLL amplitude (blue circles) and slope (red squares) on the probe power for cesium D_2 transition $F = 4 \rightarrow F'$ with fixed 70 G of axial quantification magnetic field. The corresponding linearly fits are respectively shown by the blue and red straight lines. (b) Dependences of DAVLL amplitude (blue line) and slope (red squares) on the quantification magnetic field for cesium D_2 transition $F = 4 \rightarrow F'$ with fixed 90 pW of total incident power of probe light. The corresponding linearly fits are also given.

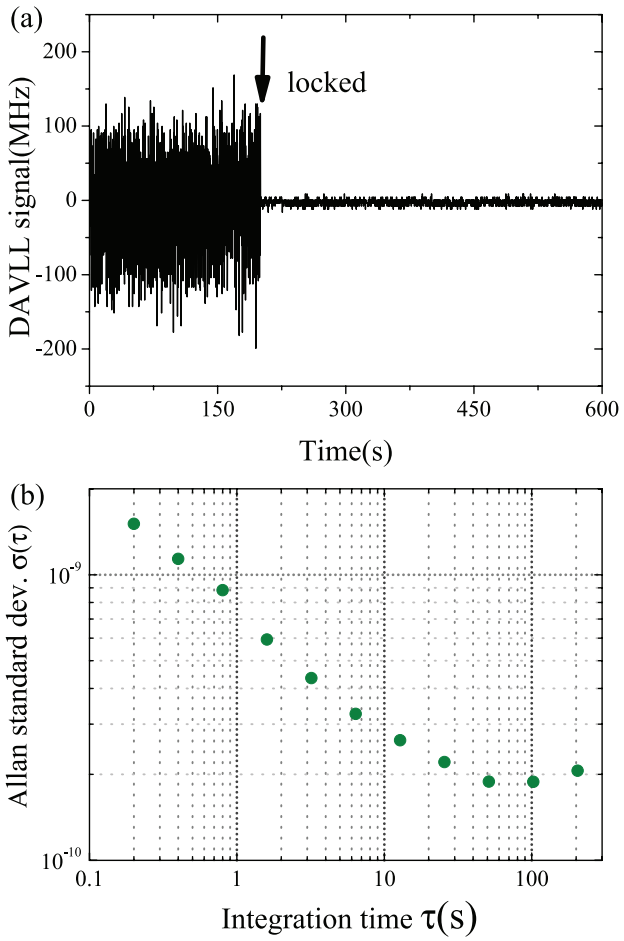

Figure 4. (a) DAVLL signal before and after locking the laser frequency. (b) The Allan standard deviation of locked laser frequency. The DAVLL signal used for frequency stabilization is obtained on the condition of total 90 pW of incident probe power and 70 G of axial quantification magnetic field strength.

scanning electron microscope (SEM), tapered nanofibers have a minimum diameter of roughly 500 nm (500 ± 10 nm) over a length of 5 mm, which agree well with the designed structure shape. Figure 1(b) shows the image obtained by the SEM. In vacuum, the tolerant power of nanofiber is over 30 mW due to its high transmission (99.5%). The tapered nanofiber is mounted to a copper chunk by UV-curable epoxy and sealed inside the vacuum chamber through Teflon feedthroughs. The temperature of vacuum chambers is held at about 80 °C by the heating tapes to increase the atomic density and optical depth. The atomic adsorption effect would generally degenerate the transmission of nanofiber lower than 1% and induce the heating effect which ultimately melts the tapered nanofiber. Instead of heating oven, we release the cesium atoms from the dispenser and successfully avoid the adsorption effect for the nanofiber.

An overview of our experimental scheme is shown in figure 1(c). A part of light is split for saturated absorption spectroscopy (SAS). The turbo pump connected with the vacuum system is used to maintain the low vacuum pressure. In presence of axial magnetic field B, the linearly polarized probe light would decompose into two circularly polarized components which interact differently with the atoms through nanofiber. For nanofiber structure, the polarization of guided light is maintained well and there is nearly no effect on the absorption spectroscopy. The DAVLL is obtained from the output of the polarimeter. Through the servo system, the laser frequency is ultimately stabilized with the filtered DAVLL signal.

With a quantization field of 70 G, the frequency of a 90 pW probe light is scanned over the whole Doppler broadened spectrum of cesium D_2 transition $F = 4 \rightarrow F'$. In figure 2, red and pink lines correspond to the two split circularly polarized components composed by the overlaps of all Zeeman splittings of hyperfine transitions $F = 4 \rightarrow F'$. The blue line indicates the subtraction of two circularly polarized components. The corresponding peak-peak amplitude and slope of DAVLL error signal are respectively 690 mV and 0.77 mV MHz^{-1}. On the topside, the SAS marked by the black line is used for frequency scaling.

3. Results and discussion

In figure 2, the transmission dips of circularly polarized components clearly show the absorption of cesium vapor through nanofiber. The probe lights are attenuated by about 66% larger than SAS 54.5% owing to the higher atomic density in saturated vapor pressure. For the absorption shape based on nanofiber, the broadened width is approximate 1000 MHz which is larger than the reference SAS 700 MHz due to both differences in Doppler broadening and transit broadening effect. In fact, considering the mean atomic velocity in hot vapor (about 200 m s^{-1}), the crossing time of a single atom through the effective optical field of nanofiber is only a few nanoseconds, much smaller than the atomic decay time (25 ns). Thus, the transit broadening effect (on the order of 100 MHz) plays a significant role in linewidth broadening.

The amplitude and slope of DAVLL signals used as error signals are both essential factors for laser frequency stabilization. To determine the minimal needed power in frequency locking through nanofiber technique, we carry out the peak-peak amplitude (blue circles) and slope (red squares) measurements on the power of incident probe light with a fixed 70 G magnetic field, which are shown in figure 3(a). The blue (red) straight line indicates the linear relationship between amplitude (slope) and incident probe light power. From figure 3(a), the measured minimal power of incident probe light is 15 pW with 94 mV for the amplitude and 0.1 mV MHz^{-1} for the slope of DAVLL signal.

To optimize the axial quantification magnetic field which is related to the DAVLL signal for frequency locking, the dependences of amplitude (blue circles) and slope (red squares) on the strength of magnetic field are also investigated, which are shown in figure 3(b). The probe light power is set at sub-nanowatt level (90 pW). The blue (red) straight line also indicates the linear relationship between amplitude (slope) and strength of magnetic field. When the quantification magnetic field is weak enough, the Zeeman splitting of all hyperfine transitions can be approximated to be linear to the strength of magnetic field, which results in a linear relationship between amplitude (slope) and strength of quantification magnetic field. Although the magnetic field is measured over 100 G, the corresponding DAVLL signals present evident distortions with increasing magnetic field owing to the differences in Zeeman splitting for different hyperfine energy levels. Thus, we choose the optimized 70 G of magnetic field for frequency stabilization, which simultaneously ensures the amplitude and avoids the distortion of the DAVLL signal.

Under the condition of 90 pW of total incident probe light and 70 G of quantification magnetic field, the diode laser is locked by the obtained DAVLL signal. Figure 4(a) shows the error signal before and after locking the laser frequency. The horizontal axis frequency is scaled by the SAS as shown in figure 2. The amplitude of error signal can be transformed into frequency according to the horizontal frequency difference between the two points of DAVLL peak-to-peak signal. The laser fluctuation is obviously reduced after closing the feedback loop with proportion integration differentiation (PID) for which the electronic noise can be ignored. The typical noise of detector (HAMAMATSU CR314-01) is about 1 mV which is nearly three orders smaller than the DAVLL amplitude. After optimizing the PID parameters for servo system, we calculate the Allan standard deviation based on the error signal to evaluate the frequency stability. As shown in figure 4(b), the frequency stability reaches 1×10^{-10} level after being locked tens of seconds, confirming the practicability in frequency stabilization by introducing new scheme which combines the conventional DAVLL and nanofiber techniques.

4. Conclusion

In conclusion, we have achieved frequency stabilization using sub-nanowatt optical power by combining the DAVLL and nanofiber technique. To optimize the axial quantification magnetic field, we investigate the dependences of DAVLL signal amplitude and slope on the strength of external magnetic field. To determine the minimal power of probe light for frequency locking, the dependences of amplitude and slope on the incident probe light power are also investigated. As seen from the measured the Allan standard deviation, the ultimate frequency stabilization decreases to the degree of 1×10^{-10} after being locked tens of seconds, which is one order worse than the conventional frequency stabilization techniques [6–12]. The reasons are principally arising from the wide absorption shape and fluctuations of DAVLL signal obtained by the nanofiber with extremely weak probe light. For a further step, by exploiting the sub-DAVLL technique with nanofiber through adding an additional pump light, the statilization of laser frequency may be improved. At last, owing to the convenience in constructing a fully fiber-based quantum network and small size in space for the nanofiber, the presented new scheme also helps for quantum optical device integration and extension.

Acknowledgments

This work was supported by National Key R&D Program of China (Grant No. 2017YFA0304203), Natural Science Foundation of China (Nos. 61675120, 11434007), NSFC Project for Excellent Research Team(No. 61121064), Shanxi Scholarship Council of China, '1331KSC', PCSIRT (No. IRT_17R70) and 111 project (Grant No. D18001).

ORCID iDs

Yan-Ting Zhao https://orcid.org/0000-0002-3343-2382

References

[1] Stern B, Ji X-C, Dutt A and Lipson M 2017 *Opt. Lett.* **42** 4541–4
[2] Zhang W-F and Yao J-P 2018 *Nat. Commun.* **9** 1396
[3] Spencer D T *et al* 2018 *Nature* **557** 81–5
[4] Poon J K S 2018 *Nat. Photon.* **12** 255–6
[5] Zi F, Wu X-J, Zhong W-C, Parker R H, Yu C-H, Budker S, Lu X-H and Muller H 2017 *Appl. Opt.* **56** 2649–52

[6] Abel R P, Mohapatra A K, Bason M G, Pritchard J D, Weatherill K J, Raitzsch U and Adams C S 2009 *Appl. Phys. Lett.* **94** 071107
[7] Tsuchida H and Iwasaki T 1992 *Opt. Lett.* **17** 49–51
[8] Duan J, Qi X-H, Zhou X-J and Chen X-Z 2011 *Opt. Lett.* **36** 561–3
[9] Parniak M, Leszczyński A and Wasilewski W 2016 *Appl. Phys. Lett.* **108** 161103
[10] Carr C, Adams C S and Weatherill K J 2012 *Opt. Lett.* **37** 118–20
[11] Corwin K L, Lu Z-T, Hand C F, Epstein R J and Wieman C E 1998 *Appl. Opt.* **37** 3295–8
[12] Su D-Q, Meng T-F, Ji Z-H, Yuan J-P, Zhao Y-T, Xiao L-T and Jia S-T 2014 *Appl. Opt.* **53** 7011–6
[13] Hoffman J E, Ravets S, Grover J A, Solano P, Kordell P R, Wong-Campos J D, Orozco L A and Rolston S L 2014 *AIP Adv.* **4** 067124
[14] Ward J M, Maimaiti A, Le V H and Chormaic S N 2014 *Rev. Sci. Instrum.* **85** 111501
[15] Nagai R and Aoki T 2014 *Opt. Express* **22** 28427–36
[16] Spillane S M, Pati G S, Salit K, Hall M, Kumar P, Beausoleil R G and Shahriar M S 2008 *Phys. Rev. Lett.* **100** 233602
[17] Watkins A, Tiwari V B, Ward J M and Chormaic S N 2013 *Proc. SPIE* **8785** 87850S
[18] Solano P, Barberis-Blostein P, Fatemi F K, Orozco L A and Rolston S L 2017 *Nat. Commun.* **8** 1857
[19] Shen J T and Fan S 2005 *Opt. Lett.* **30** 2001–3
[20] Kien F L and Rauschenbeutel A 2014 *Phys. Rev.* A **90** 063816
[21] Nayak K P, Melentiev P N, Morinaga M, Kien F L, Balykin V I and Hakuta K 2007 *Opt. Express* **15** 5431–8
[22] Lodahl P, Mahmoodian S, Stobbe S, Rauschenbeutel A, Schneeweiss P, Volz J, Pichler H and Zoller P 2017 *Nature* **541** 473–80
[23] Sayrin C, Junge C, Mitsch C C, Albrecht B, O'Shea D, Schneeweiss P, Volz J and Rauschenbeutel A 2015 *Phys. Rev.* X **5** 041036
[24] Goban A, Choi K S, Alton D J, Ding D, Lacroûte C, Pototschnig M, Thiele T, Stern N P and Kimble H J 2012 *Phys. Rev. Lett.* **109** 033603
[25] Schlosser N, Reymond G and Grangier P 2002 *Phys. Rev. Lett.* **89** 023005
[26] Sayrin C, Clausen C, Albrecht B, Schneeweisms P and Rauschenbeutel A 2015 *Optica* **2** 353–6
[27] Gouraud B, Maxein D, Nicolas A, Morin O and Laurat J 2015 *Phys. Rev. Lett.* **114** 180503
[28] Sørensen H L, Béguin J-B, Kluge K W, Iakoupov I, SØrensen A S, Müller J H, Polzik E S and Appel J 2016 *Phys. Rev. Lett.* **117** 133604
[29] Corzo N V, Gouraud B, Chandra A, Goban A, Sheremet A S, Kupriyanov D V and Laurat J 2016 *Phys. Rev. Lett.* **117** 133603
[30] Shomroni I, Rosenblum S, Lovsky Y, Bechler O, Guendelman G and Dayan B 2014 *Science* **345** 903–6
[31] Goban A, Hung C-L, Hood J D, Yu S-P, Muniz J A, Painter O and Kimble H J 2015 *Phys. Rev. Lett.* **115** 063601
[32] Hood J D, Goban A, Asenjo-Garcia A, Lu M, Yu S-P, Chang D E and Kimble H J 2016 *Proc. Natl Acad. Sci. USA* **113** 10507–12